



## Article

# Estrogen Decreases Cytoskeletal Organization by Forming an ER $\alpha$ /SHP2/c-Src Complex in Osteoclasts to Protect against Ovariectomy-Induced Bone Loss in Mice

Hyun-Jung Park <sup>1,†</sup> , Malihatosadat Gholam-Zadeh <sup>1,†</sup>, Sun-Young Yoon <sup>1</sup>, Jae-Hee Suh <sup>2</sup> and Hye-Seon Choi <sup>1,\*</sup>

<sup>1</sup> Department of Biological Sciences (BK21 Program), University of Ulsan, Ulsan 680-749, Korea; oli\_jjung@naver.com (H.-J.P.); ma\_gholamzadeh@yahoo.com (M.G.-Z.); tjsdud9981@naver.com (S.-Y.Y.)

<sup>2</sup> Department of Pathology, Ulsan University Hospital, Ulsan 682-714, Korea; drjhsuh@gmail.com

\* Correspondence: hschoi@mail.ulsan.ac.kr; Tel.: +82-52-259-1545; Fax: +82-52-259-2740

† The first two authors contributed equally to this work.

**Abstract:** Loss of ovarian function is closely related to estrogen (E<sub>2</sub>) deficiency, which is responsible for increased osteoclast (OC) differentiation and activity. We aimed to investigate the action mechanism of E<sub>2</sub> to decrease bone resorption in OCs to protect from ovariectomy (OVX)-induced bone loss in mice. In vivo, tartrate-resistant acid phosphatase (TRAP) staining in femur and serum carboxy-terminal collagen crosslinks-1 (CTX-1) were analyzed upon E<sub>2</sub> injection after OVX in mice. In vitro, OCs were analyzed by TRAP staining, actin ring formation, carboxymethylation, determination of reactive oxygen species (ROS) level, and immunoprecipitation coupled with Western blot. In vivo and in vitro, E<sub>2</sub> decreased OC size more dramatically than OC number and Methyl-piperidino-pyrazole hydrate dihydrochloride (MPPD), an estrogen receptor alpha (ER $\alpha$ ) antagonist, augmented the OC size. ER $\alpha$  was found in plasma membranes and E<sub>2</sub>/ER $\alpha$  signaling affected receptor activator of nuclear factor  $\kappa$ B ligand (RANKL)-induced actin ring formation by rapidly decreasing a proto-oncogene tyrosine-protein kinase, cellular sarcoma (c-Src) (Y416) phosphorylation in OCs. E<sub>2</sub> exposure decreased physical interactions between NADPH oxidase 1 (NOX1) and the oxidized form of c-Src homology 2 (SH2)-containing protein tyrosine phosphatase 2 (SHP2), leading to higher levels of reduced SHP2. ER $\alpha$  formed a complex with the reduced form of SHP2 and c-Src to decrease c-Src activation upon E<sub>2</sub> exposure, which blocked a signal for actin ring formation by decreased Vav guanine nucleotide exchange factor 3 (Vav3) (p-Y) and Ras-related C3 botulinum toxin substrate 1 (Rac1) (GTP) activation in OCs. E<sub>2</sub>/ER $\alpha$  signals consistently inhibited bone resorption in vitro. In conclusion, our study suggests that E<sub>2</sub>-binding to ER $\alpha$  forms a complex with SHP2/c-Src to attenuate c-Src activation that was induced upon RANKL stimulation in a non-genomic manner, resulting in an impaired actin ring formation and reducing bone resorption.

**Keywords:** estrogen (E<sub>2</sub>); ER $\alpha$ ; osteoclast; actin ring formation; non-genomic signal



**Citation:** Park, H.-J.; Gholam-Zadeh, M.; Yoon, S.-Y.; Suh, J.-H.; Choi, H.-S. Estrogen Decreases Cytoskeletal Organization by Forming an ER $\alpha$ /SHP2/c-Src Complex in Osteoclasts to Protect against Ovariectomy-Induced Bone Loss in Mice. *Antioxidants* **2021**, *10*, 619. <https://doi.org/10.3390/antiox10040619>

Academic Editor: Maria-Jose Alcaraz

Received: 23 February 2021

Accepted: 15 April 2021

Published: 17 April 2021

**Publisher's Note:** MDPI stays neutral with regard to jurisdictional claims in published maps and institutional affiliations.



**Copyright:** © 2021 by the authors. Licensee MDPI, Basel, Switzerland. This article is an open access article distributed under the terms and conditions of the Creative Commons Attribution (CC BY) license (<https://creativecommons.org/licenses/by/4.0/>).

## 1. Introduction

Within the skeleton, constant remodeling and repairing of old bones is required to ensure structural integrity. Excessive bone resorption leads to decreased bone mass, disrupted architecture, or inappropriate bone formation responses during remodeling [1]. Bone resorbing cells, osteoclasts (OCs) require two essential factors; macrophage-colony stimulating factor (M-CSF) and RANKL. M-CSF stimulates mainly OCs survival and proliferation as well as activation through cross-talking with RANKL [2]. A family member of tumor necrosis factor receptor, RANK expresses on OC precursor cells as a transmembrane signaling receptor for RANKL to result in expression of OC-specific genes, activation of bone resorption, and OC survival [3]. The degree of bone resorption reflects the number and matrix-degrading activity of OCs [4]. The number of OCs is regulated by OC differentiation as well as OC survival. While the functional activity of mature OCs in bone

resorption is mainly governed by the cytoskeletal organization of an actin ring structure that surrounds the resorption area, isolating it from the extracellular space and concentrating bone-degrading molecules. OCs express a receptor for vitronectin, integrin alpha V beta 3, which plays a critical role in cytoskeletal organization. A deficiency of  $\alpha_V\beta_3$  integrin has been reported to disrupt cytoskeletal organization, leading to increased bone mass caused by impaired bone resorption by OCs [5]. The absence of c-Src has also been demonstrated to result in impaired cytoskeletal organization, similar to the phenotype of  $\alpha_V\beta_3$  integrin-deficiency [6]. More recently, the signaling complex of c-Src/Vav3 was found to be activated upon integrin occupancy [7] to activate Rac1 [8]. RANKL has been reported to directly promote bone resorption by OC via inducing the association of c-Src with receptor activator of nuclear factor  $\kappa$ B (RANK) in an  $\alpha_V\beta_3$  integrin-dependent manner. Cross-linking of RANKL and RANK induces an interaction with  $\alpha_V\beta_3$  to induce an integrin-associated canonical pathway for actin ring formation via an axis of c-Src/Vav3/Rac1 activation [9].

Postmenopausal osteoporosis is a systemic skeletal disease involving low bone mass and deteriorated microarchitecture because of a loss of ovarian function. The decline of ovarian function has been associated with estrogen ( $E_2$ ) deficiency, which increases the formation and activity of osteoclasts (OCs). Elevated osteoclastogenesis, caused by a drop in estrogen levels, is the most common characteristic of postmenopausal osteoporosis [10,11]. Although  $E_2$  has mainly been considered to affect the attenuation of bone resorption to prevent bone loss [4,12], the detailed mechanisms involved remain to be elucidated.

In our study, we investigated an action mechanism of  $E_2$  signaling that is associated with decreased bone resorption in OCs.

## 2. Materials and Methods

### 2.1. Ethics Statement

All mice were handled following guidelines of the Institutional Animal Care and Use Committee (IACUC) of the Immunomodulation Research Center (IRC), University of Ulsan. All animal procedures were approved by the IACUC of IRC. The approval ID for this study is #HSC-19-010 (20190801).

### 2.2. Reagents and Antibodies

Recombinant mouse macrophage-colony stimulating factor (M-CSF) and receptor activator of nuclear factor  $\kappa$ B ligand (RANKL) were obtained from R and D Systems, Inc. (Minneapolis, MN, USA). Estradiol, 2',2',2'-tribromoethanol, N-acetyl-L-cysteine (NAC), and Hoechst 33258 were obtained from Sigma Chemicals (St. Louis, MO, USA). MPPD was from Tocris (Bristol, UK). Minimum essential medium  $\alpha$  ( $\alpha$ -MEM) without phenol red and MicroAmp fast reaction tubes (8 tubes/strip) were from Life Technologies (Carlsbad, CA, USA). We obtained rhodamine-phalloidin from Molecular Probes (Carlsbad, CA, USA) and N-(biotinoyl)-N'-(iodoacetyl) ethylenediamine (BIAM) from Invitrogen (Carlsbad, CA, USA). Abs against phospho-tyrosine (4G10) was purchased from Upstate USA Inc. (Charlottesville, VA, USA), and Vav guanine nucleotide exchange factor 3 (Vav3) was from Abcam (Cambridge, MA, USA). c-Src-Y416 was obtained from Cell Signaling Technology (Denver, MA, USA); c-Src homology 2 (SH2) containing protein tyrosine phosphatase 2 (SHP2), estrogen receptor  $\alpha$  ( $ER\alpha$ ), and caveolin-1 were from Santa Cruz Biotechnology (Santa Cruz, CA, USA); c-Src was sourced from ECM Biosciences (Versailles, KY, USA); NADPH oxidase 1 (NOX1) was from Novus (Centennial, CO, USA); and  $\beta$ -actin was from Sigma-Aldrich (St. Louis, MO, USA). In accordance with the manufacturer's protocol, active Ras-related C3 botulinum toxin substrate (Rac) was measured using the Rac1 activation kit from Thermo Scientific (Rockford, IL, USA). The RatLaps kit (carboxy-terminal collagen crosslinks-1; CTX-1) EIA was from Immunodiagnostic Systems Inc. (Fountain Hills, AZ, USA).

### 2.3. Animals, Culture of OCs, and OC Formation

Ten-week-old female an inbred strain, C57 black 6 J (C57BL/6 J) mice were subjected to a sham operation ( $n = 10$ ) or ovariectomy (OVX) ( $n = 12$ ) under anesthesia using 2,2,2-tribromoethanol (250 mg/kg).  $E_2$  (0.1 mg/kg) or vehicle was injected intraperitoneally and daily for 4 weeks starting 2 days after surgery. Blood was collected retro-orbitally under anesthesia before sacrifice, and tissues were harvested immediately. In vivo markers of bone resorption were measured according to the manufacturer's directions (Immunodiagnostic Systems Inc., Fountain Hills, AZ, USA) and serum CTX-1 was assessed using a RatLaps enzyme-linked immunosorbent assay (EIA). To determine TRAP-positive OCs in vivo, mouse femora were excised, cleaned with soft tissue, and decalcified in ethylenediaminetetraacetic acid (EDTA). Representative histological sections of the distal femoral metaphysis from mice in each of the four groups were stained for TRAP to identify OCs (original magnification  $\times 400$ ).

The femora and tibiae were removed aseptically and dissected to remove adherent soft tissue. The ends of the bones were cut, and the marrow cavity was flushed with  $\alpha$ -MEM from one end using a sterile 21-gauge needle. The bone marrow was further agitated using a Pasteur pipette to obtain a single-cell suspension, which was washed twice and incubated on culture plates with M-CSF (20 ng/mL) for 16 h (h). Non-adherent cells were then harvested, layered on a Ficoll–Hypaque gradient, and cultured for 2 more days, by which time large populations of adherent monocyte/macrophage-like cells had formed on the bottoms of the culture plates, as previously described [13]. The few non-adherent cells were removed by washing the dishes with phosphate-buffered saline (PBS), and the adherent cells (bone marrow-derived macrophages (BMMs)) were harvested and seeded onto culture plates. The adherent cells were analyzed as negative for a T cell coreceptor, cluster of differentiation 3 (CD3) and a member of protein tyrosine phosphatase expressed on B cells, CD45R, and positive for an M-CSF receptor, cluster of differentiation 115 (CD115) [14]. The absence of contaminating stromal cells was confirmed by the lack of cell growth in the absence of M-CSF. Additional medium containing M-CSF and RANKL (40 ng/mL) was added, and the medium was replaced on day 3. For  $E_2$  treatment in vitro, the BMMs were cultured in  $\alpha$ -MEM without phenol red containing 10% charcoal-treated fetal bovine serum (FBS) [15]. After incubation for the indicated times, the cells were fixed in 10% formalin for 10 min and stained for TRAP as described [13]. The numbers of TRAP-positive multinucleated cells (MNCs) (three or more nuclei) were recorded. The area and maximum diameter of the formed OCs were measured, and the fusion index was presented as the average number of nuclei per TRAP-positive MNC [16].

### 2.4. RNA Isolation and Quantitative Polymerase Chain Reaction (qPCR)

Total RNA was isolated using QIAzol reagent. The first-strand cDNA was reverse-transcribed with random primers and Moloney murine leukemia virus (M-MLV) reverse transcriptase as described in Park et al. [17]. qPCR was carried out using SYBR green real-time PCR master mixes and the appropriate primers. Relative gene expression was calculated using the formula  $2^{-\Delta\Delta C_t}$  with normalization to ribosomal protein small subunit (RPS) gene that has been known for housekeeping [18]. The primer sequences were used as described [17].

### 2.5. Actin Cytoskeleton

To examine the actin ring within the OCs, mature OCs were cultured for 4 h under the indicated conditions as described in Kim et al. [19]. The slides were treated with 0.1% Triton X-100 in PBS for 5 min and stained with rhodamine-phalloidin for actin and Hoechst33258 for the nuclei. The cytoplasmic distribution of nuclei and F-actin were examined using an Olympus FV1200 confocal microscope (Olympus, Tokyo, Japan).

## 2.6. Western Blot Analysis

Cultured cells were harvested after washing with ice-cold PBS and then lysed in extraction buffer (50 mM Tris-HCl, pH 8.0, 150 mM NaCl, 1 mM EDTA, 0.5% Nonidet P-40, 0.01% protease inhibitor mixture). The protein concentration was determined using bicinchoninic acid (BCA) assay. Cell extracts (20 µg) were subjected to sodium dodecyl sulfate–polyacrylamide gel electrophoresis (SDS–PAGE) and transferred onto nitrocellulose membranes. Membranes were blocked for 1 h with skim milk in Tris-buffered saline containing 0.1% Tween-20 and incubated overnight at 4 °C [17] with antibodies (Ab) against c-Src-Y416, c-Src, and β-actin. An active pull-down and detection kit was used to extract and detect active Rac1 (89856Y), as directed by the manufacturer. The lysate (200 µg) was subjected to immunoprecipitation with 1 µg of antibody against Vav3, ERα, c-Src, or SHP2, followed by Western blot analysis using the corresponding Ab as indicated. Membranes were washed, incubated for 1 h with horseradish peroxidase (HRP)-conjugated secondary antibodies, and developed using chemiluminescence substrates. The original images for Western blots have been provided (Supplementary Figures S1–S3).

## 2.7. Detection of Oxidized SHP2 by Carboxymethylation

BMMs were incubated with M-CSF (30 ng/mL) and RANKL (40 ng/mL) for 55 h and further incubated in the presence or absence of E<sub>2</sub> (5 nM) for 16 h. The medium was removed, and the cells were frozen rapidly in liquid nitrogen. The frozen cells were transferred to 100 µM *N*-(biotinoyl)-*N*'-(iodoacetyl) ethylenediamine (BIAM)-containing lysis buffer (50 mM Tris-HCl, pH 7.5, 150 mM NaCl, 0.5% Triton X-100, 10 µg/mL aprotinin, and 10 µg/mL leupeptin; rendered oxygen-free by bubbling nitrogen gas through the buffer at a low flow rate for 20 min). Sulfhydryl modifying chemical BIAM selectively detects the reduced form of cysteine [20]. After sonication in a bath sonicator for three 1-min periods, the lysate was clarified by centrifugation and subjected to immunoprecipitation with 1 µg of Ab against SHP2. Immunocomplexes labeled with BIAM were detected with HRP-conjugated streptavidin, and the color was developed with an enhanced chemiluminescence kit.

## 2.8. Flow-Cytometric Quantification of Intracellular Reactive Oxygen Species (ROS)

The intracellular ROS was detected using the fluorescent probe, 2',7'-dichlorofluorescein diacetate (H<sub>2</sub>DCFDA) [21]. Incubated cells in the presence or absence of E<sub>2</sub> (5 nM), MPPD (2 µM) for 16 h, washed thoroughly, stained with H<sub>2</sub>DCFDA at 37 °C for 30 min. Intracellular ROS was measured by fluorescence-activated cell sorting (FACS) Calibur flow cytometer (Becton Dickinson, Franklin Lakes, NJ, USA).

## 2.9. Bone Resorption

OCs were further characterized by assessing their ability to form pits on dentine slices, as described in an earlier report [17]. To this end, mature OCs, which were generated by treating BMMs with M-CSF (30 ng/mL) and RANKL (40 ng/mL), were seeded on dentine slices and further incubated with E<sub>2</sub> or MPPD for another 3 days. Cells were fixed with formalin and stained for TRAP. Then, the cells were removed by ultrasonication in 1 M NH<sub>4</sub>OH and stained with 1% (*w/v*) toluidine blue in 0.5% sodium borate to visualize resorption pits. The resorption pit area was measured with ImageJ software, 1.37v.

## 2.10. Statistical Analysis

Values are expressed as means of triplicate experiments ± standard deviation (SD). Each series of experiments was repeated at least three times. Statistical analysis was performed by Student's *t*-test when two groups were compared. Two-way analysis of variance (ANOVA) was used when two variables were analyzed. A *p*-value of less than 0.05 was considered statistically significant.

### 3. Results

#### 3.1. E<sub>2</sub> Decreases Number and Size of OCs during Bone Loss in OVX Mice

To investigate the role of E<sub>2</sub> in OVX-induced bone loss, we evaluated the effect of E<sub>2</sub> on OCs from E<sub>2</sub>-injected OVX mice. In vivo, TRAP-staining showed that E<sub>2</sub> significantly decreased OC surface area divided by total bone surface area (OC.S/BS), which increased after 4 weeks of OVX with a modest decrease in OC number divided by total bone surface (OC.N/BS) (Figure 1A). A similar pattern was observed in vivo with the bone-resorption marker, serum CTX-1 (Figure 1B).

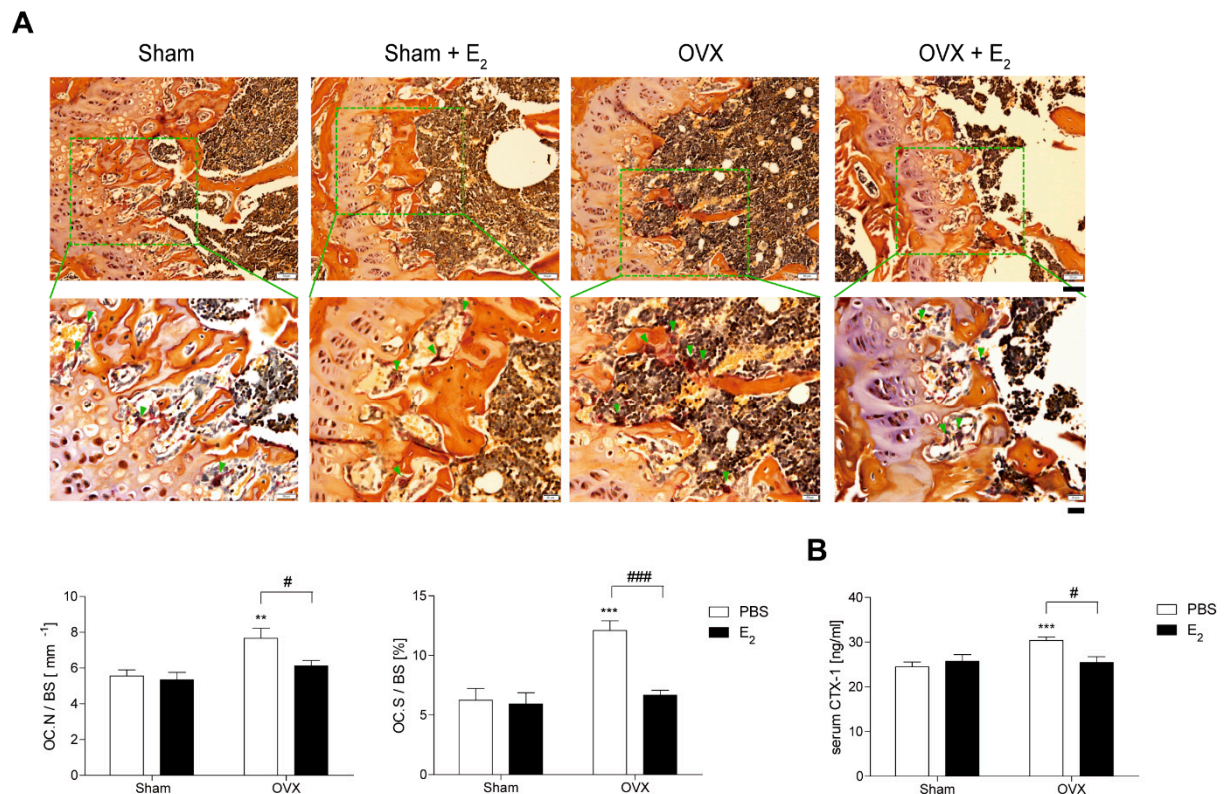


**Figure 1.** E<sub>2</sub> decreases number and size of osteoclasts (OCs) during bone loss in ovariectomy (OVX) mice. **(A)** Representative histological sections of the distal femoral metaphysis of mice from each of the 4 groups were stained for tartrate-resistant acid phosphatase (TRAP) to identify OCs (indicated by arrows) to calculate OC surface area divided by total bone surface area (OC.S/BS) and OC number divided by total bone surface (OC.N/BS). Scale bar in the representative photos: 50  $\mu$ m. Inset shows higher magnification (scale bar: 20  $\mu$ m). **(B)** Serum carboxy-terminal collagen crosslinks-1 (CTX-1) in vivo bone resorption marker. \*\*  $p < 0.01$ ; \*\*\*  $p < 0.001$  compared with sham mice. #  $p < 0.05$ ; ###  $p < 0.001$  compared with PBS-injected mice. Two-way ANOVA, followed by Bonferroni posttests was used to compare the effect of E<sub>2</sub> (OC.N/BS and serum CTX-1;  $p < 0.05$ , OC.S/BS;  $p < 0.001$ ), the effect of surgery (serum CTX-1;  $p < 0.05$ , OC.N/BS;  $p < 0.01$ , OC.S/BS;  $p < 0.001$ ) and interactions (OC.S/BS;  $p < 0.01$ , serum CTX-1;  $p < 0.05$ ) (A,B).

#### 3.2. E<sub>2</sub> Inhibits NUMBER and Size of OCs during Osteoclast Differentiation

To assess the effect of E<sub>2</sub> on OC differentiation in vitro, we determined the expression of OC-specific genes on RANKL stimulation after 48 h of exposure to E<sub>2</sub>. As shown in Figure 2A, E<sub>2</sub> exposure did not change the RANKL-induced OC differentiation-associated genes expression levels, including TRAP, nuclear factors of activated T cells 2 (NFAT2), calcineurin- and calcium-regulated transcription factor, and the lysosomal proteolytic enzyme cathepsin K [2,3]. To confirm that E<sub>2</sub> acts in the late stages of osteoclastogenesis, we added E<sub>2</sub> to OC cultures after 55 h exposure of RANKL. E<sub>2</sub> decreased the number of OCs, the OC area, and fusion index at the late-stage and had profound effects on OC size, compared to number and fusion index (Figure 2B). Next, we assessed which cytokine signal was specific to E<sub>2</sub> exposure. The effect of E<sub>2</sub> on the OC area was more dramatic upon

RANKL stimulation, whereas there was no significant effect of E<sub>2</sub> on M-CSF stimulation (Figure 2C). Conversely, blocking the E<sub>2</sub> signal with the ER $\alpha$  antagonist, MPPD, increased OC area and fusion index without any change in the OC number (Figure 2C). MPPD more efficiently augmented OC area than it did fusion index and number of OCs.

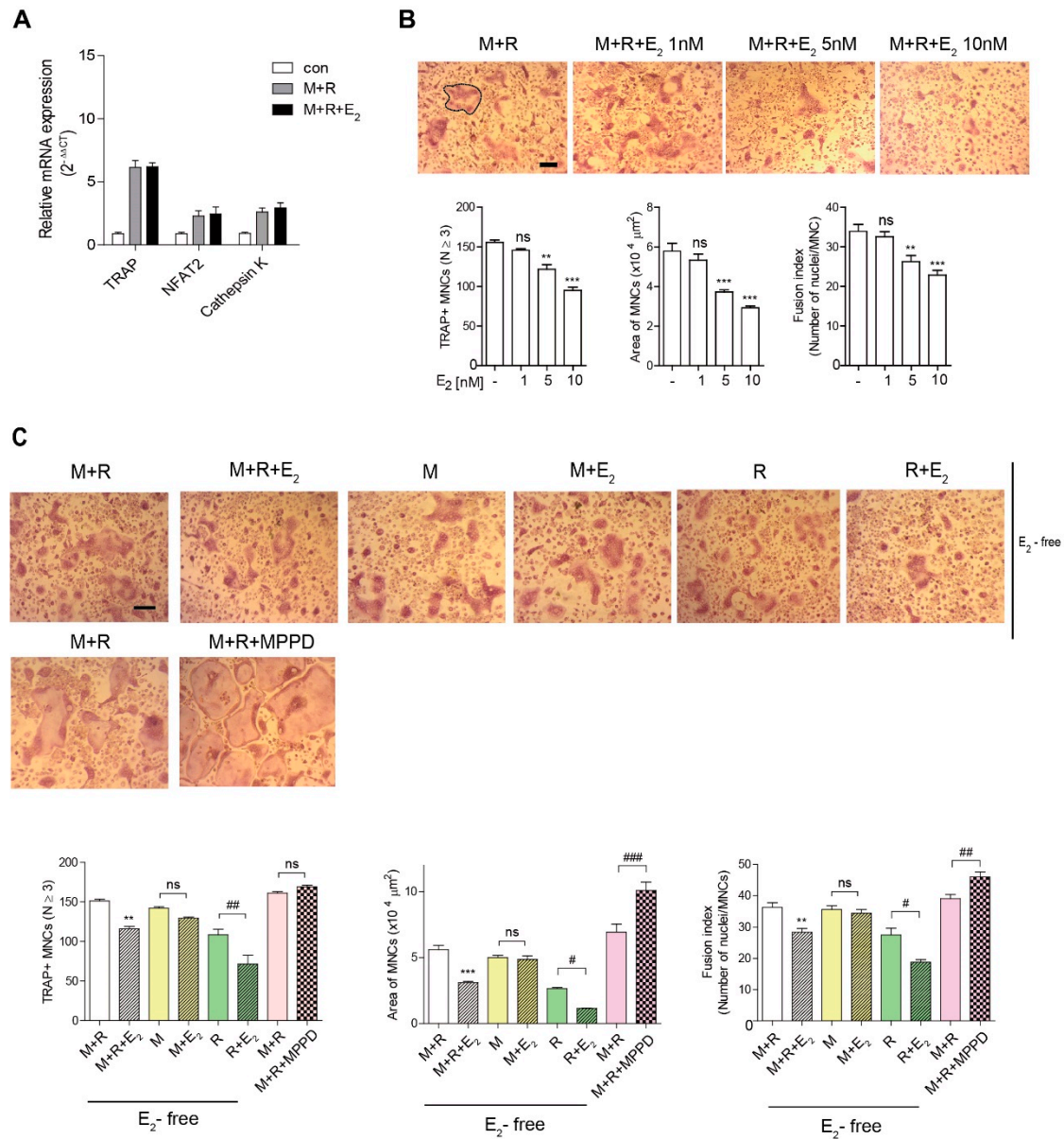


**Figure 2.** E<sub>2</sub> inhibits the number and size of OCs during osteoclast differentiation in vitro. (A) RNA from bone marrow-derived macrophages (BMMs) cultured with M-CSF (30 ng/mL) and receptor activator of nuclear factor κB ligand (RANKL) (40 ng/mL) in the presence of E<sub>2</sub> (5 nM) for 48 h was analyzed by qPCR. The expression level before RANKL treatment was set to 1. (B,C) BMMs were cultured with M-CSF (30 ng/mL) and RANKL (40 ng/mL) for 5 h, and then E<sub>2</sub> (1 nM, 5 nM, 10 nM) (B) or MPPD (2 μM) (C) was added for another 16 h upon M-CSF and/or RANKL to determine TRAP-positive multinucleated cells (MNCs). After cells were fixed, more than 70 TRAP-positive MNCs in each culture were randomly selected. The area of formed OCs surrounded by the bold line was measured. The fusion index presented is the average number of nuclei per TRAP-positive MNC formed in the culture. Representative photos are shown. Scale bar in the representative OC photos: 100 μm. \*\* *p* < 0.01; \*\*\* *p* < 0.001 compared with vehicle group. # *p* < 0.05; ## *p* < 0.01; ### *p* < 0.001 compared with each corresponding control. Similar results were obtained in three independent experiments.

### 3.3. E<sub>2</sub> Inhibits RANKL-Stimulated Actin Ring Formation

To confirm whether E<sub>2</sub> affects OC spreading by impairing actin cytoskeletal reorganization, we evaluated whether E<sub>2</sub> inhibits the actin ring formation essential for bone resorption in OCs. Mature OCs were generated on a plastic well and incubated with M-CSF or RANKL in the presence or absence of E<sub>2</sub>, and the cells were stained with rhodamine-phalloidin to visualize the actin ring. As shown in Figure 3A, the removal of cytokines completely abolished actin ring-containing OCs, whereas the addition of M-CSF and RANKL recovered the number of actin ring-containing cells. However, E<sub>2</sub> reduced it. The effect of E<sub>2</sub> on actin-ring formation was more prominent with RANKL stimulation, whereas no significant effect was observed with M-CSF stimulation. In contrast, MPPD treatment increased the number of OCs having actin rings (Figure 3B).

### 3.4. E<sub>2</sub> Transmits Signaling by Forming an ER $\alpha$ /c-Src/SHP2 Complex, Resulting in Disrupted c-Src Activation in a Non-Genomic Manner

Because E<sub>2</sub> more potently blocked RANKL-induced actin ring formation in OCs, we evaluated the effect of E<sub>2</sub> on RANKL-stimulated signaling pathways that mediate cytoskeletal reorganization. RANKL-induced c-Src activation was evaluated by the phosphorylation of c-Src-Y416. E<sub>2</sub> has been reported to transmit hormonal signals through genomic or non-genomic mechanisms [22–24]; therefore, we determined the times required for E<sub>2</sub> to decrease c-Src activation. As shown in Figure 4A, E<sub>2</sub> significantly reduced the amount of phosphorylated c-Src as early as 1 min exposure. Whereas the ER $\alpha$  antagonist, MPPD, increased phosphorylated c-Src (Supplementary Figure S1). Western blot analysis combined with co-immunoprecipitation showed a direct interaction between ER $\alpha$  and caveolin-1, a plasma membrane marker, in the absence or presence of E<sub>2</sub> in OCs (Figure 4B, Supplementary Figure S1). Next, we determined whether ER $\alpha$  associates with c-Src to generate an E<sub>2</sub> response upon RANKL stimulation in OCs. As shown in the top panel of Figure 5A, co-immunoprecipitation demonstrated that the direct interaction between ER $\alpha$  and c-Src upon RANKL stimulation was enhanced after E<sub>2</sub> exposure, whereas it was attenuated upon MPPD treatment. Since tyrosine phosphatase is required to decrease c-Src activation, and SHP2 has been demonstrated to have a physical association with ER $\alpha$  [23], we evaluated whether this is the case when E<sub>2</sub> was added in RANKL-stimulated OCs. As we expected, there was an increased association between SHP2 and ER $\alpha$  upon E<sub>2</sub> exposure. The opposite result was observed with MPPD treatment (Figure 5A, Supplementary Figure S2). E<sub>2</sub> was then shown to enhance the direct interaction between c-Src and SHP2 in the co-immunoprecipitation experiment with SHP2, followed by binding of c-Src, (Figure 5B, left, Supplementary Figure S2). The same phenomenon was observed with immunoprecipitation with c-Src and immunoblotting with SHP2 (Figure 5B, right, Supplementary Figure S2). Next, to investigate how the activity of SHP2 is regulated, we evaluated whether ROS affects the activity of SHP2 via oxidation. We labeled the cell with BIAM, which is a sulfhydryl-modifying reagent that exhibits selective binding with the thiolate form of reduced cysteine (Cys) residues. SHP2 was immunoprecipitated and biotinylated, and reduced fractions of SHP2 were conjugated with HRP–streptavidin. As shown in Figure 5C, SHP2 was oxidized upon RANKL stimulation, as there were decreased levels of the reduced form of SHP2, whereas E<sub>2</sub> exposure reversed this effect. MPPD increased the oxidization of SHP2, whereas *N*-acetyl cysteine (NAC), a ROS scavenger, decreased it as a positive control (Supplementary Figure S2). Then, to find out the potential molecule that contributes to converting SHP2 by ROS generation, we examined whether SHP2 was modulated by its interaction with NOX1 upon E<sub>2</sub> exposure. As shown in Figure 5D, RANKL induced a direct interaction between SHP2 and NOX1, whereas E<sub>2</sub> decreased their association. The opposite was seen with MPPD treatment. However, NOX1 did not interact with c-Src in the presence of E<sub>2</sub> or MPPD (Supplementary Figure S2). Next, we determined ROS generated from NOX1 upon exposure to E<sub>2</sub> or MPPD to assess the activity of NOX1. RANKL alone increased ROS, whereas the addition of E<sub>2</sub> decreased it, and MPPD reversed it (Figure 5E).

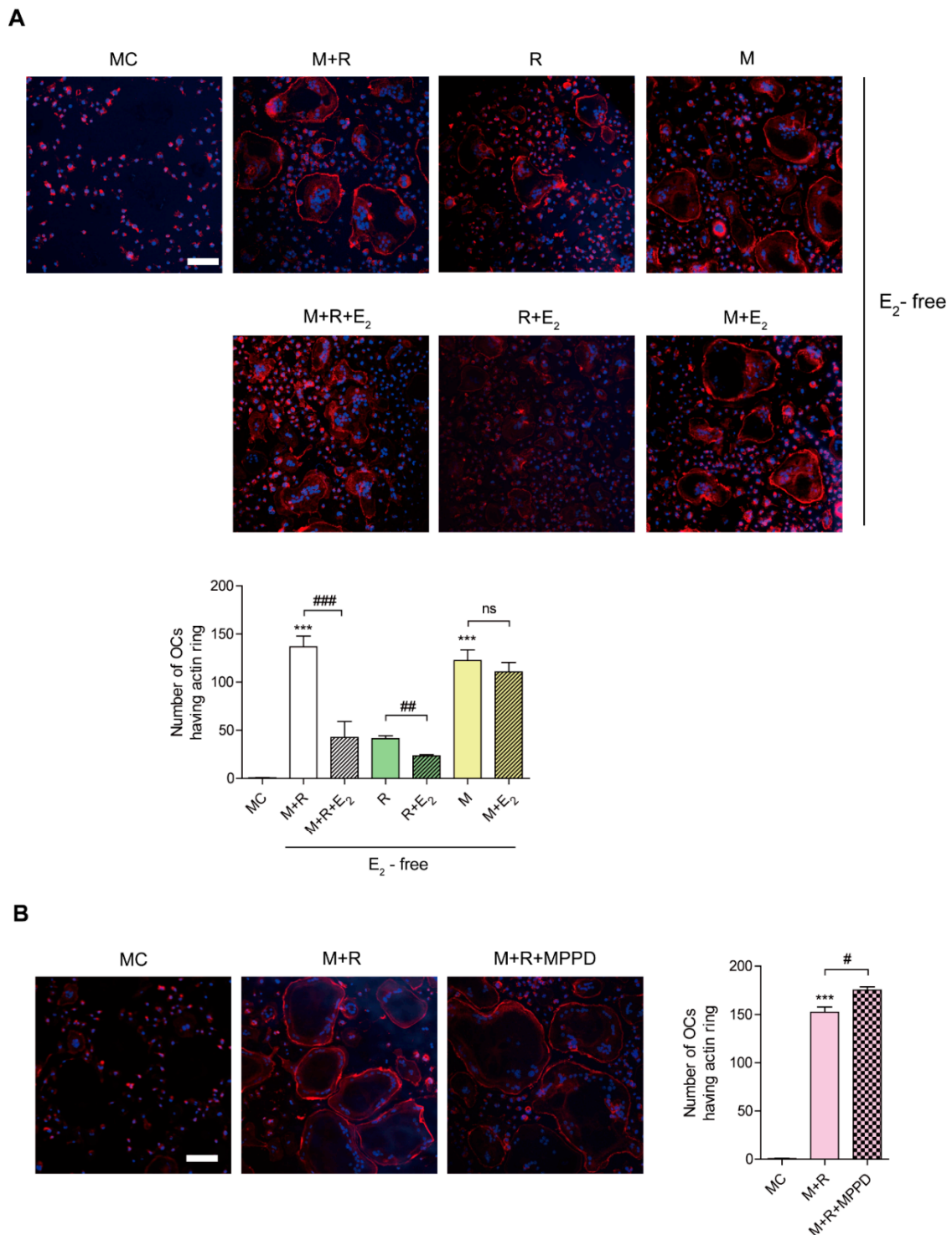


**Figure 3.** E<sub>2</sub> inhibits RANKL-stimulated actin ring formation. BMMs were cultured with M-CSF (30 ng/mL) and RANKL (40 ng/mL) for 96 h. **(A)** Cells were incubated with  $\alpha$ -MEM/10% FBS (media control, MC) or with E<sub>2</sub> (5 nM) in the presence of M-CSF (M, 30 ng/mL) and/or RANKL (R, 40 ng/mL) as indicated. **(B)** Cells were incubated with  $\alpha$ -MEM/10% FBS (media control, MC) or with MPPD (2  $\mu$ M) in the presence of M-CSF and RANKL. After a 4 h incubation, the cells were stained with rhodamine–phalloidin and Hoechst to visualize actin ring and nuclei, respectively. **(A,B)** show representative images. Scale bar, 100  $\mu$ m. The number of OCs having actin rings was plotted for the indicated conditions. \*\*\*  $p < 0.001$  compared with MC. #  $p < 0.05$ ; ##  $p < 0.01$ ; ###  $p < 0.001$  compared with each corresponding control. Similar results were obtained in three independent experiments.

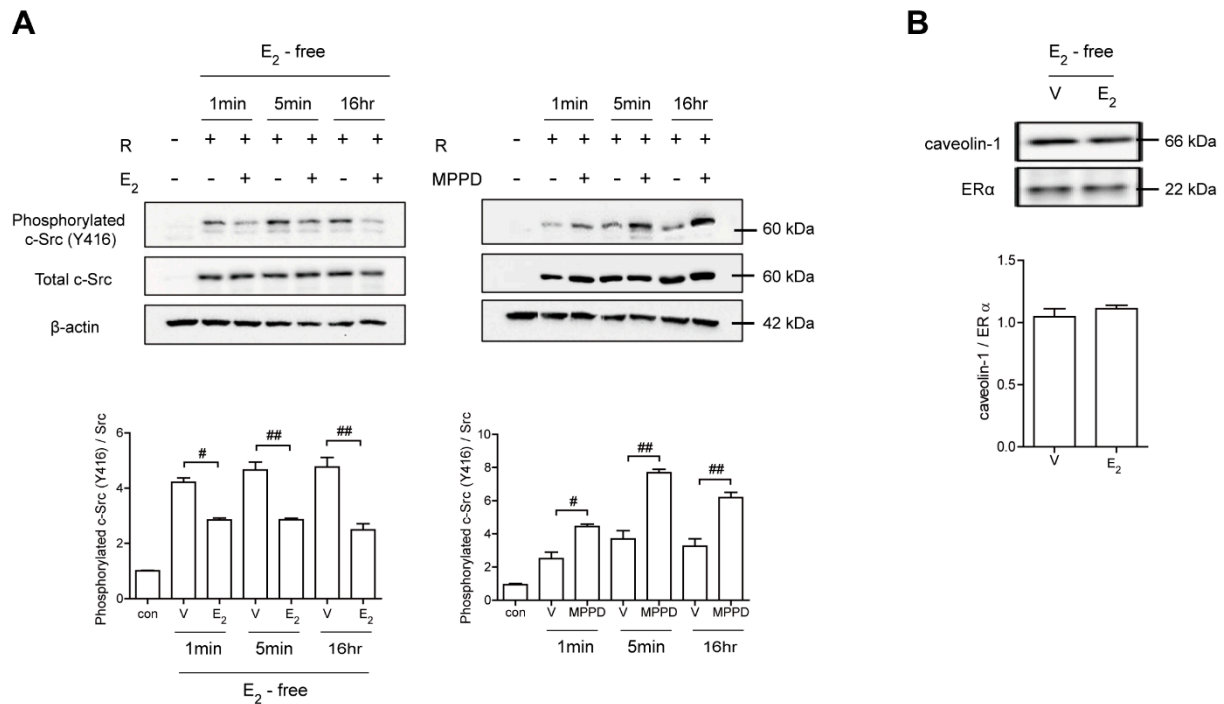


**Figure 4.** E<sub>2</sub> transmits signaling via ERα, resulting in disrupted c-Src activation in a non-genomic manner. BMMs stimulated with RANKL (50 ng/mL) in the absence and presence of E<sub>2</sub> (5 nM) or MPPD (2 μM) for the indicated time. (A) The cell lysate was immunoblotted for phosphorylated c-Src (Y416). (B) Cell lysates were prepared for co-immunoprecipitation with specific antibodies to ERα and subjected to immunoblotting as indicated. # *p* < 0.05; ## *p* < 0.01 compared with each corresponding control. Similar results were obtained in three independent experiments.

### 3.5. E<sub>2</sub> Inhibits RANKL-Induced Cytoskeletal Reorganization via an Axis of c-Src/Vav3/Rac1, Leading to Decreased Bone Resorption

Next, we assessed whether decreased c-Src activation is transmitted to block activations of Vav3 and Rac1 to affect actin ring formation. Vav3 has been reported to be an OC-specific guanidine nucleotide exchange factor that targets Rac1 [25]. Consistent with its effect on c-Src, E<sub>2</sub> attenuated the tyrosine phosphorylation of Vav3 induced by RANKL (Figure 6A, Supplementary Figure S3). Rac1 activation was assessed using a glutathione-S-transferase (GST) pull-down assay. While Rac1 activation was enhanced after 5 min exposure to RANKL, it was reduced by the addition of E<sub>2</sub> compared with RANKL alone (Figure 6B, Supplementary Figure S3). Consistent with its morphological and functional phenotypes, E<sub>2</sub> suppressed the major cytoskeleton-organizing signals by decreasing c-Src/Vav3/Rac1 signaling in OCs.

To determine whether E<sub>2</sub> affects OC activity, we assessed the effect of E<sub>2</sub> on bone resorption using dentine slices. As shown in Figure 6C, mature OCs generated with M-CSF and RANKL were mounted on dentine slices with/without E<sub>2</sub> in the presence of cytokines. The addition of E<sub>2</sub> resulted in significantly reduced OC total pit area/OC number compared with cells stimulated with cytokines only, whereas MPPD increased it (Figure 6C).

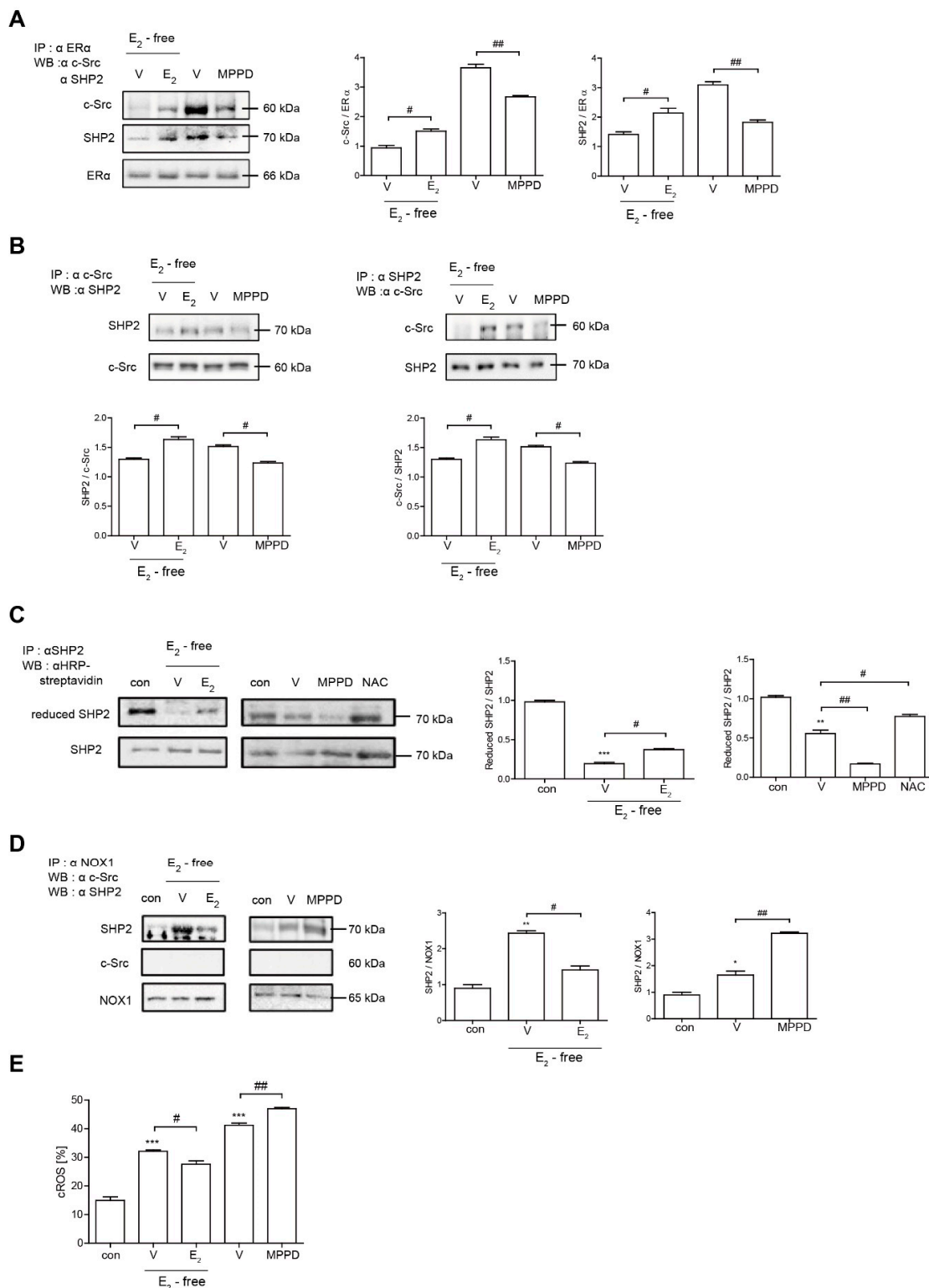


**Figure 5.**  $E_2$  transmits signaling by forming an ER $\alpha$ /c-Src/SHP2 complex to decrease c-Src activation. (A,B,D) Cell lysates were prepared for co-immunoprecipitation with specific antibodies to ER $\alpha$ , c-Src, SHP2, or NOX1 and subjected to immunoblotting as indicated. (C) After labeling of cell lysate using BIAM, immunoprecipitation (IP) was performed with anti-SHP2, followed by HRP–streptavidin immunoblotting to isolate the reduced form of SHP2. (E) BMMs were cultured with M-CSF and RANKL for 55 h, and then  $E_2$  (5 nM) or MPPD (2  $\mu$ M) was added for another 16 h upon M-CSF and/or RANKL to determine cytosolic ROS level. \*  $p < 0.05$ ; \*\*  $p < 0.01$ ; \*\*\*  $p < 0.001$  compared with control. #  $p < 0.05$ ; ##  $p < 0.01$  compared with each corresponding control. Similar results were obtained in three independent experiments.

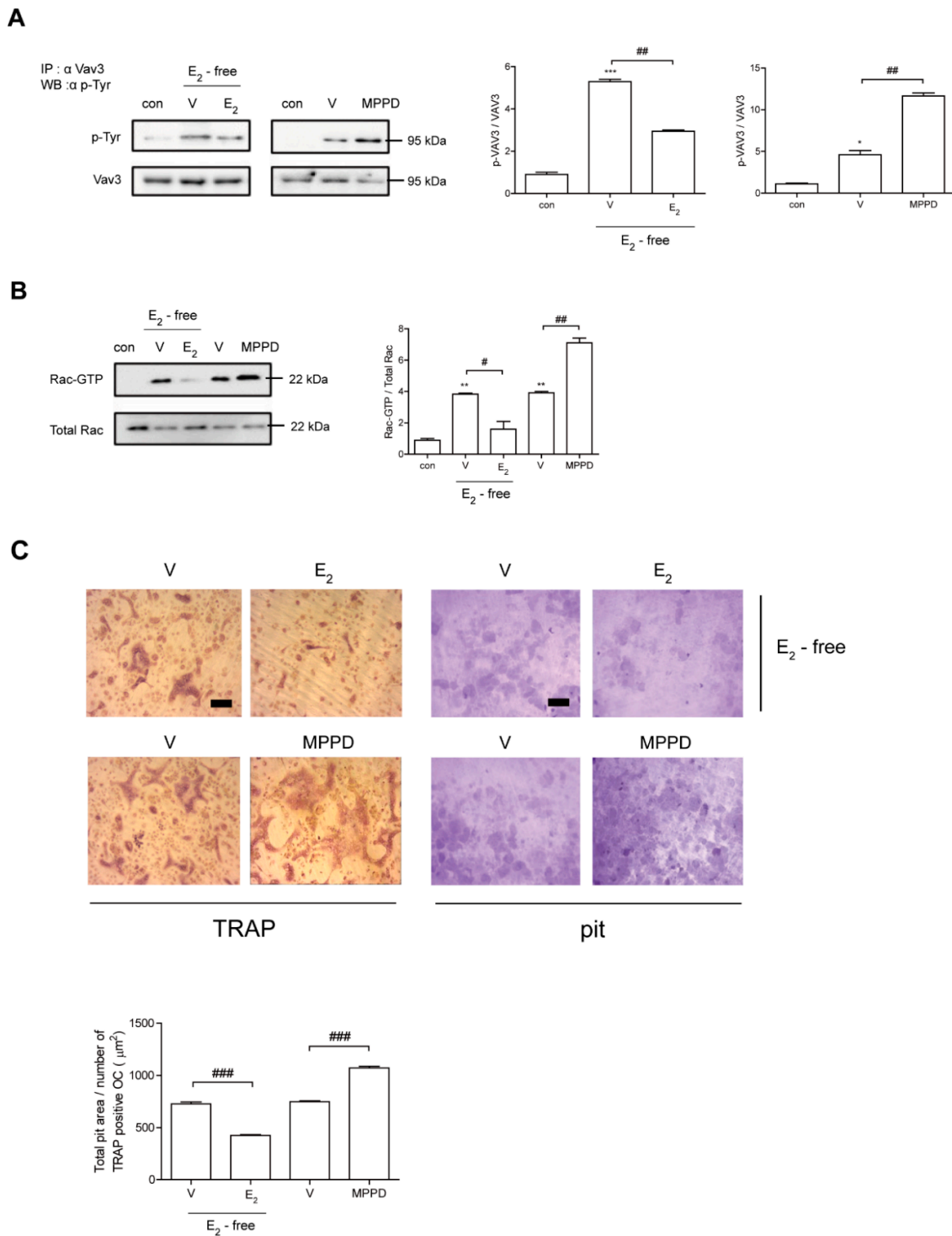


**Figure 6.**  $E_2$  inhibits RANKL-induced cytoskeletal reorganization via an axis of c-Src/Vav3/Rac1, leading to decreased bone resorption. (A) Vav3 was immunoprecipitated from cell lysate, and the phosphotyrosine (p-Tyr) content of the immunoprecipitate was determined by immunoblot with anti-phosphotyrosine Ab. (B) GTP-Rac was isolated by GST pull-down and immunoblotted with Rac-specific Ab. (C) Mature OCs were incubated further on whole dentine slices with M-CSF and RANKL in the presence or absence of  $E_2$  (5 nM) or MPPD (2  $\mu\text{M}$ ) for 3 days. After TRAP staining, the cells were removed, and the slices were stained with toluidine blue. Representative photos of TRAP-positive OCs and resorption pits are shown. Scale bar in the representative photos: 100  $\mu\text{m}$ . The total pit area/number of TRAP-positive OCs was calculated. \*  $p < 0.05$ ; \*\*  $p < 0.01$ ; \*\*\*  $p < 0.001$  compared with control. #  $p < 0.05$ ; ##  $p < 0.01$ ; ###  $p < 0.001$  compared with each corresponding control. Similar results were obtained in three independent experiments.

#### 4. Discussion

We have demonstrated the mechanisms by which  $E_2$  affects the OC to recover OVX-induced bone loss.  $E_2$  did not change the expression of OC-specific genes, such as TRAP, NFAT2, and cathepsin K, suggesting that the early stages of OC differentiation were not affected by  $E_2$ . However,  $E_2$  decreased the cell area more prominently than it did the number and fusion index of OCs, while the opposite pattern was observed with the ER $\alpha$  antagonist, MPPD, implying the possibility that  $E_2$ /ER $\alpha$  signaling may reduce OC spreading via disrupted cytoskeletal reorganization. As we expected,  $E_2$  impaired actin ring formation. The signaling through  $E_2$ /ER $\alpha$  was affected upon RANKL stimulation but not upon M-CSF stimulation, suggesting that impaired OC spreading by  $E_2$  signals could be RANKL-dependent. Our data demonstrated that  $E_2$  decreased RANKL-induced signaling for cytoskeletal reorganization through blocking the activation of c-Src/Vav3/Rac1, an effect that also has been reported for RANKL stimulation [9]. After 1 min of  $E_2$  exposure, the level of phosphorylated c-Src-Y416 was diminished, suggesting that the signaling was transmitted rapidly. In addition, the co-immunoprecipitation assay showed there was an interaction between ER $\alpha$  and caveolin-1, a plasma membrane marker, indicating ER $\alpha$  is located on plasma membranes. Those findings suggested that the inhibitory effect of  $E_2$  during RANKL-induced c-Src activation occurred in a non-genomic way. Although ERs belong to the nuclear receptor protein family, which regulates the expression of target genes by binding DNA at specific response elements, many studies have demonstrated these receptors to have secondary signaling roles transmitted in a non-genomic way [22–24]. In agreement with our results,  $E_2$  exhibits rapid cellular responses in a non-nuclear manner, acting through receptors found in cell membranes as well as in the cytoplasm [22]. The rapid signaling of  $E_2$ , via the association between ER $\alpha$  and c-Src, also has been demonstrated in endothelial cells [24].

The protective effects of  $E_2$  in bone loss have been reported to occur through OCs [26,27]. OC-specific ER $\alpha$ -knockout mice exhibited a similar phenotype to that of osteoporotic women with low trabecular bone density and failed to show further bone loss upon loss of ovarian function [27]. In the absence of ER $\alpha$ , mature OCs are resistant to the apoptotic effects of  $E_2$ , implying that the main role of  $E_2$  in OCs is to enhance apoptosis and thereby increase bone density [27]. In agreement with this, the effect of  $E_2$  on bone resorption has been suggested to involve inducing OCs to directly carry out apoptosis [28,29]. However, our results demonstrated that  $E_2$  more potently decreased OC activity by impairing cytoskeletal organization than it did OC number under the assayed conditions. Our results corroborate those of several studies that found  $E_2$  affects the cytoskeleton in OCs [30,31]. The absence of Siglec-15 exhibited resistance to  $E_2$  deficiency-induced bone loss with OCs that failed to spread onto the bone surface, indicating that  $E_2$  is associated with cytoskeleton organization via Siglec-15 in OCs [30]. Genistein, a phytoestrogen, disrupted actin ring formation by elevating cytosolic  $Ca^{2+}$  concentrations, resulting in attenuated bone resorption in rat OCs [31].

We demonstrated the detailed molecular mechanism of how  $E_2$  disrupted cytoskeletal reorganization in OCs.  $E_2$  enhanced the physical association between c-Src and the reduced (active) form of SHP2.  $E_2$ /ER $\alpha$  formed a complex with c-Src and SHP2, resulting in the dephosphorylation of Y416 of c-Src. Thus, the direct coupling of ER $\alpha$  to both c-Src and SHP2 acted to dampen the signaling event triggered by RANKL. The positive role of SHP2 in mediating  $E_2$  signaling by forming an SHP2/ER $\alpha$  complex has been reported in the modulation of body weight and energy balance in conjunction with leptin [23]. In addition, the SHP2 effect was enhanced in Shp<sup>D61A</sup> mutants that have increased catalytic activity [23], suggesting the important role of SHP2 activity in  $E_2$ /ER $\alpha$  signaling. We hypothesized that ROS modulates SHP2 activity via its interaction with NOX1 demonstrated to be induced upon RANKL stimulation [32]. The assays of the immunoprecipitation, carboxymethylation, and ROS level showed that RANKL stimulation increased a direct interaction between NOX1 and SHP2 inactive ROS-induced oxidation, whereas  $E_2$  exposure reversed it. A similar pattern was found with NAC, suggesting the effect of  $E_2$  was mediated by decreased

ROS levels. Taken together, the results showed that  $E_2/ER\alpha$  transmits the signal to form a complex with active SHP2 and c-Src due to decreased interaction between NOX1 and inactive SHP2, finally leading to attenuating c-Src activation upon RANKL stimulation.

Although  $E_2$  exhibits strong protective effects against postmenopausal osteoporosis in clinical studies, its therapeutic application has been limited due to its side effects [33]. Our results suggest that SHP2 or NOX1 acts as a downstream molecule to exhibit the  $E_2$  effect in OCs. Currently, the number of SHP2 inhibitors are under clinical trials for tumor-targeted therapies [34] and NAC as a ROS scavenger has been reported to improve traumatic brain injury in human trials [35], suggesting an implication for their therapeutic application as an alternative to  $E_2$  for bone loss in human.

## 5. Conclusions

Our present findings suggest that  $E_2$  binding to  $ER\alpha$  formed a complex with active SHP2 and c-Src to attenuate RANKL-stimulated c-Src activation due to decreased interaction between NOX1 and inactive SHP2 in a non-genomic way. Dephosphorylation of c-Src was followed by the blockade of Vav3 and Rac1 activation by RANKL stimulation (Figure 7). This resulted in impaired actin ring formation in OCs and, therefore, reduced bone resorption. Our results demonstrate the novel action mechanism of  $E_2$  in OCs to impair cytoskeletal reorganization in a non-genomic way, suggesting that SHP2 or NOX1 could be a potential therapeutic target for osteoporosis upon loss of ovarian function.

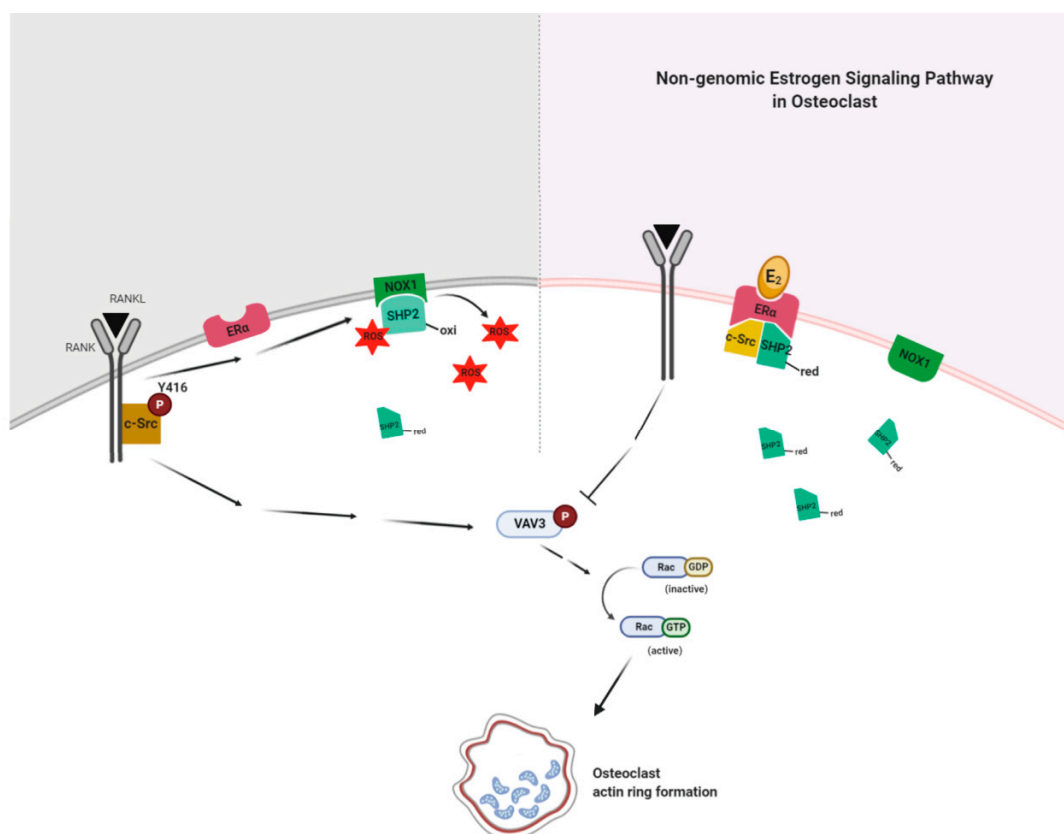


**Figure 7.**  $E_2$  signaling plays a critical role in an impaired actin ring formation. RANKL activates c-Src and transmits a signal to generate reactive oxygen species (ROS) via NADPH oxidase 1 (NOX1), resulting in the association of NOX1 and the oxidized form (inactive) of c-Src homology 2 (SH2)-containing protein tyrosine phosphatase 2 (SHP2) to decrease the availability of the reduced (active) form of SHP2.  $E_2$  binding to  $ER\alpha$  forms a complex with active SHP2 and c-Src to attenuate RANKL-stimulated c-Src activation due to increased availability of the reduced form of SHP2 through the decreased interaction between NOX1 and the oxidized form of SHP2 in a non-genomic way. Dephosphorylation of c-Src is followed by the blockade of Vav3 and Rac1 activation by RANKL stimulation. This results in impaired actin ring formation in OCs and, therefore, reduced bone resorption.

**Supplementary Materials:** The following are available online at <https://www.mdpi.com/article/10.3390/antiox10040619/s1>, Figure S1: Raw data of western blot for Figure 4, Figure S2: Raw data of western blot for Figure 5, and Figure S3: Raw data of western blot for Figure 6.

**Author Contributions:** The study was designed by H.-J.P., M.G.-Z., and H.-S.C. and was performed by H.-J.P., M.G.-Z., S.-Y.Y., and J.-H.S. The manuscript was written by H.-J.P., M.G.-Z., and H.-S.C. All authors have read and agreed to the published version of the manuscript.

**Funding:** This work was supported by the National Research Foundation of Korea (NRF) grants Basic Science Research Programs of the NRF funded by the Korea government (2021R1A2C1003423; 2018R1A2B6001276; 2014R1A6A1030318).

**Institutional Review Board Statement:** All mice were handled following guidelines of the Institutional Animal Care and Use Committee (IACUC) of the Immunomodulation Research Center (IRC), University of Ulsan. All animal procedures were approved by the IACUC of IRC. The approval ID for this study is #HSC-19-010.

**Informed Consent Statement:** Not applicable.

**Data Availability Statement:** All original images and data are contained within the article.

**Conflicts of Interest:** The authors state that they have no conflict of interest. The funders had no role in the design of the study, analysis or interpretation of data, writing of the manuscript, or decision to publish the results.

## References

- Raisz, L.G. Pathogenesis of osteoporosis: Concepts, conflicts, and prospects. *J. Clin. Investig.* **2005**, *115*, 3318–3325. [[CrossRef](#)]
- Feng, X.; Teitelbaum, S.L. Osteoclasts: New Insights. *Bone Res.* **2013**, *1*, 11–26.
- Boyle, W.J.; Simonet, W.S.; Lacey, D.L. Osteoclast differentiation and activation. *Nature* **2003**, *423*, 337–342. [[CrossRef](#)] [[PubMed](#)]
- Teitelbaum, S.L. Osteoclasts: What do they do and how do they do it? *Am. J. Pathol.* **2007**, *170*, 427–435. [[CrossRef](#)] [[PubMed](#)]
- McHugh, K.P.; Hodivala-Dilke, K.; Zheng, M.H.; Namba, N.; Lam, J.; Novack, D.; Feng, X.; Ross, F.P.; Hynes, R.O.; Teitelbaum, S.L. Mice lacking beta3 integrins are osteosclerotic because of dysfunctional osteoclasts. *J. Clin. Investig.* **2000**, *105*, 433–440. [[CrossRef](#)]
- Soriano, P.; Montgomery, C.; Geske, R.; Bradley, A. Targeted disruption of the c-src proto-oncogene leads to osteopetrosis in mice. *Cell* **1991**, *64*, 693–702. [[CrossRef](#)]
- Faccio, R.; Novack, D.V.; Zallone, A.; Ross, F.P.; Teitelbaum, S.L. Dynamic changes in the osteoclast cytoskeleton in response to growth factors and cell attachment are controlled by beta3 integrin. *J. Cell Biol.* **2003**, *162*, 499–509. [[CrossRef](#)]
- Croke, M.; Ross, F.P.; Korhonen, M.; Williams, D.A.; Zou, W.; Teitelbaum, S.L. Rac deletion in osteoclasts causes severe osteopetrosis. *J. Cell Sci.* **2011**, *124*, 3811–3821. [[CrossRef](#)]
- Izawa, T.; Zou, W.; Chappel, J.C.; Ashley, J.W.; Feng, X.; Teitelbaum, S.L. c-Src links a RANK/ $\alpha$ v $\beta$ 3 integrin complex to the osteoclast cytoskeleton. *Mol. Cell Biol.* **2012**, *32*, 2943–2953. [[CrossRef](#)]
- Rachner, T.D.; Khosla, S.; Hofbauer, L.C. Osteoporosis: Now and the future. *Lancet* **2011**, *377*, 1276–1287. [[CrossRef](#)]
- Manolagas, S.C. From estrogen-centric to aging and oxidative stress: A revised perspective of the pathogenesis of osteoporosis. *Endocr. Rev.* **2010**, *31*, 266–300. [[CrossRef](#)] [[PubMed](#)]
- Selby, P.L.; Peacock, M.; Barkworth, S.A.; Brown, W.B.; Taylor, G.A. Early effects of ethinyloestradiol and norethisterone treatment in post-menopausal women on bone resorption and calcium regulating hormones. *Clin. Sci.* **1985**, *69*, 265–271. [[CrossRef](#)] [[PubMed](#)]
- Ke, K.; Sul, O.J.; Rajasekaran, M.; Choi, H.S. MicroRNA-183 increases osteoclastogenesis by repressing heme oxygenase-1. *Bone* **2015**, *81*, 237–246. [[CrossRef](#)]
- Arai, F.; Miyamoto, T.; Ohneda, O.; Inada, T.; Sudo, T.; Brasel, K.; Miyata, T.; Anderson, D.M.; Suda, T. Commitment and differentiation of osteoclast precursor cells by the sequential expression of c-Fms and receptor activator of nuclear factor kappaB (RANK) receptors. *J. Exp. Med.* **1999**, *190*, 1741–1754. [[CrossRef](#)]
- De Faria, A.N.; Zancanela, D.C.; Ramos, A.P.; Torqueti, M.R.; Ciancaglini, P. Estrogen and phenol red free medium for osteoblast culture: Study of the mineralization ability. *Cytotechnology* **2016**, *68*, 1623–1632. [[CrossRef](#)] [[PubMed](#)]
- Okayasu, M.; Nakayachi, M.; Hayashida, C.; Ito, J.; Kaneda, T.; Masuhara, M.; Suda, N.; Sato, T.; Hakeda, Y. Low-density lipoprotein receptor deficiency causes impaired osteoclastogenesis and increased bone mass in mice because of defect in osteoclastic cell-cell fusion. *J. Biol. Chem.* **2012**, *287*, 19229–19241. [[CrossRef](#)]
- Park, H.J.; Son, H.J.; Sul, O.J.; Suh, J.H.; Choi, H.S. 4-Phenylbutyric acid protects against lipopolysaccharide-induced bone loss by modulating autophagy in osteoclasts. *Biochem. Pharmacol.* **2018**, *151*, 9–17. [[CrossRef](#)]
- De Jonge, H.J.M.; Fehrmann, R.S.N.; de Bont, E.S.J.; Hofstra, R.M.W.; Gerbens, F.; Kamps, W.A.; de Vries, E.G.E.; van der Zee, A.G.J.; te Meerman, G.J.; ter Elst, A. Evidence Based Selection of Housekeeping Genes. *PLoS ONE* **2007**, *2*, e898. [[CrossRef](#)]

19. Kim, H.J.; Zhao, H.; Kitaura, H.; Bhattacharyya, S.; Brewer, J.A.; Muglia, L.J.; Ross, F.P.; Teitelbaum, S.L. Glucocorticoids suppress bone formation via the osteoclast. *J. Clin. Investig.* **2006**, *116*, 2152–2160. [[CrossRef](#)]
20. Giannoni, E.; Buricchi, F.; Raugei, G.; Ramponi, G.; Chiarugi, P. Intracellular reactive oxygen species activate Src tyrosine kinase during cell adhesion and anchorage-dependent cell growth. *Mol. Cell Biol.* **2005**, *25*, 6391–6403. [[CrossRef](#)]
21. Park, H.J.; Gholam-Zadeh, M.; Suh, J.H.; Choi, H.S. Lycorine Attenuates Autophagy in Osteoclasts via an Axis of mROS/TRPML1/TFEB to Reduce LPS-Induced Bone Loss. *Oxid. Med. Cell Longev.* **2019**, 8982147. [[CrossRef](#)]
22. Puglisi, R.; Mattia, G.; Carè, A.; Marano, G.; Malorni, W.; Matarrese, P. Non-genomic Effects of Estrogen on Cell Homeostasis and Remodeling With Special Focus on Cardiac Ischemia/Reperfusion Injury. *Front. Endocrinol.* **2019**, *10*, 1–18. [[CrossRef](#)]
23. He, Z.; Zhang, S.S.; Meng, Q.; Li, S.; Zhu, H.H.; Raquil, M.A.; Alderson, N.; Zhang, H.; Wu, J.; Rui, L.; et al. Shp2 Controls Female Body Weight and Energy Balance by Integrating Leptin and Estrogen Signals. *Mol. Cell Biol.* **2012**, *32*, 1867–1878. [[CrossRef](#)]
24. Haynes, M.P.; Li, L.; Sinha, D.; Russell, K.S.; Hisamoto, K.; Baron, R.; Collinge, M.; Sessa, W.C.; Bender, J.R. Src kinase mediates phosphatidylinositol 3-kinase/Akt-dependent rapid endothelial nitric-oxide synthase activation by estrogen. *J. Biol. Chem.* **2003**, *278*, 2118–2123. [[CrossRef](#)] [[PubMed](#)]
25. Faccio, R.; Teitelbaum, S.L.; Fujikawa, K.; Chappel, J.; Zallone, A.; Tybulewicz, V.L.; Ross, F.P.; Swat, W. Vav3 regulates osteoclast function and bone mass. *Nat. Med.* **2005**, *11*, 284–290. [[CrossRef](#)] [[PubMed](#)]
26. Lean, J.M.; Davies, J.T.; Fuller, K.; Jagger, C.J.; Kirstein, B.; Partington, G.A.; Urry, Z.L.; Chambers, T.J. A crucial role for thiol antioxidants in estrogen-deficiency bone loss. *J. Clin. Investig.* **2003**, *112*, 915–923. [[CrossRef](#)] [[PubMed](#)]
27. Martin-Millan, M.; Almeida, M.; Ambrogini, E.; Han, L.; Zhao, H.; Weinstein, R.S.; Jilka, R.L.; O'Brien, C.A.; Manolagas, S.C. The estrogen receptor- $\alpha$  in osteoclasts mediates the protective effects of estrogens on cancellous but not cortical bone. *Mol. Endocrinol.* **2010**, *24*, 323–334. [[CrossRef](#)] [[PubMed](#)]
28. Kameda, T.; Mano, H.; Yuasa, T.; Mori, Y.; Miyazawa, K.; Shiokawa, M.; Nakamaru, Y.; Hiroi, E.; Hiura, K.; Kameda, A.; et al. Estrogen inhibits bone resorption by directly inducing apoptosis of the bone-resorbing osteoclasts. *J. Exp. Med.* **1997**, *186*, 489–495. [[CrossRef](#)]
29. Hughes, D.E.; Dai, A.; Tiffée, J.C.; Li, H.H.; Mundy, G.R.; Boyce, B.F. Estrogen promotes apoptosis of murine osteoclasts mediated by TGF- $\beta$ . *Nat. Med.* **1996**, *2*, 1132–1136. [[CrossRef](#)]
30. Kameda, Y.; Takahata, M.; Mikuni, S.; Shimizu, T.; Hamano, H.; Angata, T.; Hatakeyama, S.; Kinjo, M.; Iwasaki, N. Siglec-15 is a potential therapeutic target for postmenopausal osteoporosis. *Bone* **2015**, *71*, 217–226. [[CrossRef](#)]
31. Kajiya, H.; Okabe, K.; Okamoto, F.; Tsuzuki, T.; Soeda, H. Protein tyrosine kinase inhibitors increase cytosolic calcium and inhibit actin organization as resorbing activity in rat osteoclasts. *J. Cell Physiol.* **2000**, *183*, 83–90. [[CrossRef](#)]
32. Lee, N.K.; Choi, Y.G.; Baik, J.Y.; Han, S.Y.; Jeong, D.; Bae, Y.S.; Kim, N.; Lee, S.Y. A crucial role for reactive oxygen species in RANKL-induced osteoclast differentiation. *Blood* **2005**, *106*, 852–859. [[CrossRef](#)]
33. Stepan, J.J.; Hruskova, H.; Kverka, M. Update on Menopausal Hormone Therapy for Fracture Prevention. *Curr. Osteoporos. Rep.* **2019**, *17*, 465–473. [[CrossRef](#)] [[PubMed](#)]
34. Song, Z.; Wang, M.; Ge, Y.; Chen, X.P.; Xu, Z.; Sun, Y.; Xiong, X.F. Tyrosine phosphatase SHP2 inhibitors in tumor-targeted therapies. *Acta Pharmacol. Sin. B* **2021**, *11*, 13–29. [[CrossRef](#)] [[PubMed](#)]
35. Bhatti, J.; Nascimento, B.; Akhtar, U.; Rhind, S.G.; Tien, H.; Nathens, A.; da Luz, L.T. Systematic Review of Human and Animal Studies Examining the Efficacy and Safety of N-Acetylcysteine (NAC) and N-Acetylcysteine Amide (NACA) in Traumatic Brain Injury: Impact on Neurofunctional Outcome and Biomarkers of Oxidative Stress and Inflammation. *Front. Neurol.* **2017**, *8*, 744. [[CrossRef](#)] [[PubMed](#)]